Supplementary Information for

Zika virus employs the host antiviral RNase L protein to support replication factory assembly

Jillian N Whelan[a], Nicholas A Parenti[a], Joshua Hatterschide[a], David M Renner[a], Yize Li[a#], Hanako M Reyes[a], Beihua Dong[b], Erick R Perez[a], Robert H Silverman[b], and Susan R Weiss[a*]

Susan R. Weiss
weisssr@pennmedicine.upenn.edu

This PDF file includes:

Supplementary text
Figures S1 to S8
SI References

Supplementary Information Text

Materials and Methods

Cells and viruses

A549 and A549 HILO cells were grown in Roswell Park Memorial Institute media 1640 (Gibco 11875) supplemented with L-Glutamine and 10% (vol/vol) fetal bovine serum (FBS, Hyclone®). Vero cells were grown in Dulbecco's modified eagle's media (DMEM, Gibco 11965) supplemented with 4.5g/L D-Glucose, 10% FBS, 10mM HEPES, 1mM sodium pyruvate, and 50µg/mL gentamicin (Gibco). A549 OAS1 KO, OAS2 KO, OAS3 KO, and two RNase L KO clones were generated as previously described (1, 2). HeLa M cells expressing pcDNA3 vector, RNase L WT, or RNase L nuclease dead mutant R667A (3) were cultured in DMEM supplemented with 10% FBS. Zika virus 2015 Puerto Rico isolate PRVABC59 (KX377337) and Dengue virus type 2 (DENV2, New Guinea C, bei resources) were obtained from Dr. Scott Hensley, University of Pennsylvania, Philadelphia, and were propagated in Vero cells. West Nile virus Kunjin strain MRM61C was provided by Dr. Sara Cherry, University of Pennsylvania, Philadelphia, originally obtained from Dr. Alexander Khromykh, University of Queensland, Australia (4), and propagated in BHK-21 cells.

Generation of doxycycline-inducible RNase L A549 HILO cells

We constructed a pLenti-CRISPR-sgRNase L plasmid using a previously described single guide RNA (sgRNA) targeting human *RNASEL* (1). The doxycycline-inducible A549 HILO-RMCE cell system has been previously described (5). A549 HILO acceptor cells, donor pRD and pCAGGS-Cre plasmids were provided by Dr. Matthew Weitzman, University of Pennsylvania, Philadelphia. We used the pLenti-CRISPR-sgRNase L plasmid and our previously described CRISPR-Cas9 gene editing procedure to delete RNase L from A549 HILO-RMCE acceptor cells (A549 HILO RL KO), selecting cells with hygromycin and single cell cloning (6). We cloned flag-tagged RNase L WT or RNase L R667A catalytic mutant (3, 7) into RMCE donor plasmid pRD using AgeI and BsrGI restriction sites, and transfected them into A549 HILO RL KO cells with pCAGGS-Cre. Cells were selected with 1.5ug/mL puromycin. RNase L expression was induced with 2μg/mL doxycycline for 24h before cells were infected with ZIKV at indicated MOI and length of time. See Figure S6.

Virus replication assays

Cells were seeded into 24-well plates and infected the next day at indicated MOI in triplicate. After 1h incubation of cells with virus at 37°C, virus was removed and cells washed three times with PBS before addition of 1mL complete media. At indicated time post-infection, 150µl supernatants were harvested and stored at -80°C until titration, and 150µl complete

media replaced in each well so that all time points from one replicate contain supernatant from the same infected well throughout the time course. Data is representative of 2 or more experiments.

Plaque assays

Virus supernatant from infected cells was serially diluted in DMEM supplemented with 2% FBS and added to Vero cell monolayers in 6-well plates. Plates were incubated for 1 hour at 37°C before overlaying infected monolayers with DMEM containing 3% FBS, 8% $NaCO_3$, 10mM HEPES, 1X L-glutamine, 250μg/mL amphotericin B, and 0.7% agarose. Plaques were stained with neutral red after 4 days (ZIKV) or 5 days (DENV and KUNV) for 16-18h before counting plaques. Viral titers for each triplicate were calculated as plaque forming units per mL (PFU/mL) of supernatant and as the mean of duplicates. All viral titers are displayed in Log_{10} scale as the mean ± SD.

rRNA degradation assay

A549 cells were mock infected or infected with indicated virus at indicated MOI for the indicated number of hours. Cells were harvested in RLT buffer (RNeasy Mini Kit, Qiagen) and lysed through a QIAshredder (Qiagen). Total RNA was extracted and ribosomal RNA integrity was analyzed on RNA microchips using an Agilent 2100 BioAnalyzer (8, 9). RNA integrity number (RIN) quantified total eukaryotic RNA degradation, with 1 being the most degraded and 10 being the most intact.

Immunofluorescence assays

Cells were seeded onto glass coverslips in 12-well plates and the next day mock infected or infected with ZIKV at an MOI of 1. Cells were fixed with 10% formalin at indicated timepoint post-infection (20hpi except for S1A), permeablized with 0.1% triton X-100 in PBS for 15 minutes, and blocked with bovine serum albumin (BSA) for 1h. Coverslips were incubated in primary then secondary antibody diluted in 1% BSA for 1h at RT, with three PBS washes after each antibody. Mouse anti-dsRNA antibody (J2, Scicons) was diluted at 1:500, rabbit anti-protein disulfide-isomerase (PDI, Cell Signaling C81H6) for labeling ER was used at 1:200, rabbit anti-βtubulin (Cell Signaling 9F3) was used at 1:200, and rabbit anti-ZIKV NS3 (GeneTex 133320) was used at 1:1,500. Goat anti-mouse Alexa fluor® 488 (Invitrogen A11029) and goat anti-rabbit Alexa fluor® 594 (Invitrogen A11037) secondary antibodies displayed as green and red stains, respectively, were used at 1:400. Cells were briefly incubated with 4′,6-diamidino-2-phenylindole (DAPI) to stain nuclei, then rinsed with PBS. Coverslips were mounted onto glass slides and sealed using ProLong Gold antifade reagent (Invitrogen P36930), and imaged using a Nikon Ti2E fluorescence widefield microscope at 60X (Figure 5) or 100X magnification (Figure S1), or using a VT-iSIM confocal microscope at 100X magnification (all other IFA images). Images shown are representative of 5 or more fields of view taken per condition, for each of 2 or more independent experiments. All images within individual experiments were batch

processed using the same contrast and threshold settings before measurement. IFAs for quantification were imaged on a Nikon Ti2E fluorescence widefield microscope at 20X magnification.

Fluorescence *in situ* hybridization

A549 cells were seeded onto 8-well chamber slides (EMD Millipore) and the next day infected with ZIKV at an MOI of 1. At indicated timepoint, cells were fixed with 10% formalin for 30 minutes at RT, dehydrated, rehydrated, treated with protease and stained with fluorescent labels specific to positive-strand ZIKV genome (cat 521511), positive-strand DENV genome (cat 528001), or positive-strand West Nile virus genome (cat 475091) using RNAscope® Fluorescent Multiplex Reagent Kit (Advanced Cell Diagnostics, Inc.). After FISH staining, slides were rinsed with ddH_2O, rinsed with PBS, then blocked with BSA and stained for PDI or dsRNA as described for IFAs, using goat anti-rabbit Alexa fluor® 488 (Invitrogen A11005) secondary antibody for green ER or dsRNA staining. RNA was imaged on at 60X on a Nikon Ti2E fluorescence widefield microscope (Figure 5) or a VT-iSIM confocal microscope at 100X magnification. Images shown are representative of 5 or more fields of view taken per condition, for each of 2 or more independent experiments. All images within individual experiments were batch processed using the same contrast and threshold settings before measurement. Images for quantification were taken on a Nikon Ti2E fluorescence widefield microscope at 20X magnification.

Image quantification

IFA and FISH images for quantification were taken on a Nikon Ti2E fluorescence widefield microscope at 20X magnification. Scatter dot plots shown are representative of at least two individual experiments with >100 infected cells measured per sample, from at least five fields taken per condition, with mean displayed as a black bar. For IFA quantification, images were processed for quantification using ImageJ/FIJI by setting a threshold to define the regions of interest (ROIs) as individual RFs (labeled by dsRNA or NS3). Mean intensity was calculated by measuring the mean gray value within ROIs (RFs). Circularity was calculated using the formula 4pi(area/perimeter^2), where an RF in the shape of a perfect circle results in a value of 1. Feret's diameter, also known as the maximum caliper, is the largest distance between two points on the perimeter of the RF. Mean gray value, circularity, area, and Feret's diameter are standard measures of ROIs in ImageJ/FIJI. For FISH images, ROIs contained all RNA throughout each individual cell. Since viral RNA ROIs did not take on a defined shape, a perimeter around each ROI was drawn manually, and area of the ROI measured. Relative fluorescence units (RFU) for intensity, microns for Feret's diameter, and $microns^2$ for area are displayed on the y-axis. Circularity measurements do not have a unit and are reported as arbitrary units (AU).

2-5A fluorescence resonance energy transfer (FRET) assays

A549 cells seeded into 6-well plates were infected the next day with ZIKV at an MOI of 5, or mock infected. After 24h, cells were washed with PBS and scraped off of the plate, centrifuged at 1,000 x *g* for 15 minutes at 4°C. PBS was aspirated, and 200μl NP-40 (1%) buffer pre-heated at 95°C for 2 minutes was added to pellet. Samples were further processed as described (10) and assayed for 2-5A levels by FRET assays as described (11).

pIC transfection

Cells were seeded in 24-well plates, with coverslips if for FISH + IFA, and the next day transfected ± 250ng/mL pIC using Lipofectamine 2000 (Invitrogen) for 2h prior to infection with ZIKV at MOI 1. Cells not treated with pIC were transfected with Lipofectamine only. Cells were either fixed for IFAs at 24hpi or supernatant for replication curves was harvested at 2 and 24hpi for downstream analysis.

Paclitaxel treatment

Paclitaxel (Sigma-Aldrich) was resuspended in dimethylsulfoxide (DMSO). Cells were infected with ZIKV at an MOI of 1 for 3h before paclitaxel or DMSO was added to cell supernatant at a final concentration of 12.5μM, as described in (12). Cells were fixed or supernatant harvested for downstream analysis.

Western blotting

Whole cell lysate was boiled for 10 minutes at 95°C, loaded onto pre-cast 10% polyacrylamide gels (Bio-Rad), migrated through the gel by SDS-PAGE at 110V, transferred onto PVDF membrane (EMD Millipore) for 3h at 150mA, blocked in 5% milk overnight, incubated in primary and HRP-conjugated secondary antibodies in 5% milk for 1h each incubation, and imaged using chemiluminescent HRP substrate (Thermo Scientific™ SuperSignal™ West Pico). Goat anti-OAS3 N-18 (Santa Cruz) was used at 1:250, mouse anti-human RNase L (13) at 1:1000, mouse anti-flavivirus envelope (E) protein (Novus Biologicals D1-4G2-4-15) at 1:500, rabbit anti-ZIKV NS3 (GeneTex GTX133309) at 1:1000, rabbit anti-DENV NS3 (GeneTex GTX124252) at 1:1000, mouse anti-FLAG (Sigma M2 F1804) at 1:1000, and mouse anti-GAPDH as a loading control at 1:1000 (Thermo Fisher MA5-15738).

RT-qPCR

A549 cells were seeded into 24-well plates and the next day infected with indicated virus at an MOI of 1 for 20h. Cells were harvested in RLT buffer (RNeasy Plus Mini Kit, Qiagen), lysed through a QIAshredder (Qiagen), and DNase-treated. Total RNA was extracted and 200ng RNA was reverse transcribed into cDNA with SuperScript™ III 4 (Invitrogen). cDNA was amplified using virus-specific RT-qPCR primers, iQ™ SYBR® Green Supermix (Bio-Rad), and the QuantStudio™ 3 PCR system (Thermo Fisher). Primers amplifying 18S rRNA, and ZIKV and DENV genome have been previously described (6). The West Nile virus Kunjin strain primers were: forward-TGGACGGGGAATACCGACTTAGAGG, and reverse-

ACCCCAGCTGCTGCCACCTT (14). Cycle threshold (C_T) values were normalized to 18S rRNA to generate ΔC_T values (ΔC_T = C_T gene of interest - C_T 18S rRNA). Technical triplicates were averaged and displayed using the equation $2^{-(\Delta CT)}$.

Statistical analyses

All analyses were performed in GraphPad Prism version 8.2.1. Plaque assay data comparing WT and RNase L KO groups only were analyzed by student's paired t test. Image quantification data comparing WT and RNase L KO groups only were analyzed by student's unpaired t test. Plaque assay and image quantification data comparing three or more groups, and 2-5A FRET assay data were analyzed by one-way ANOVA. ns = not significant, *p<0.05, **p<0.01, ***p<0.001, ****p<0.0001.

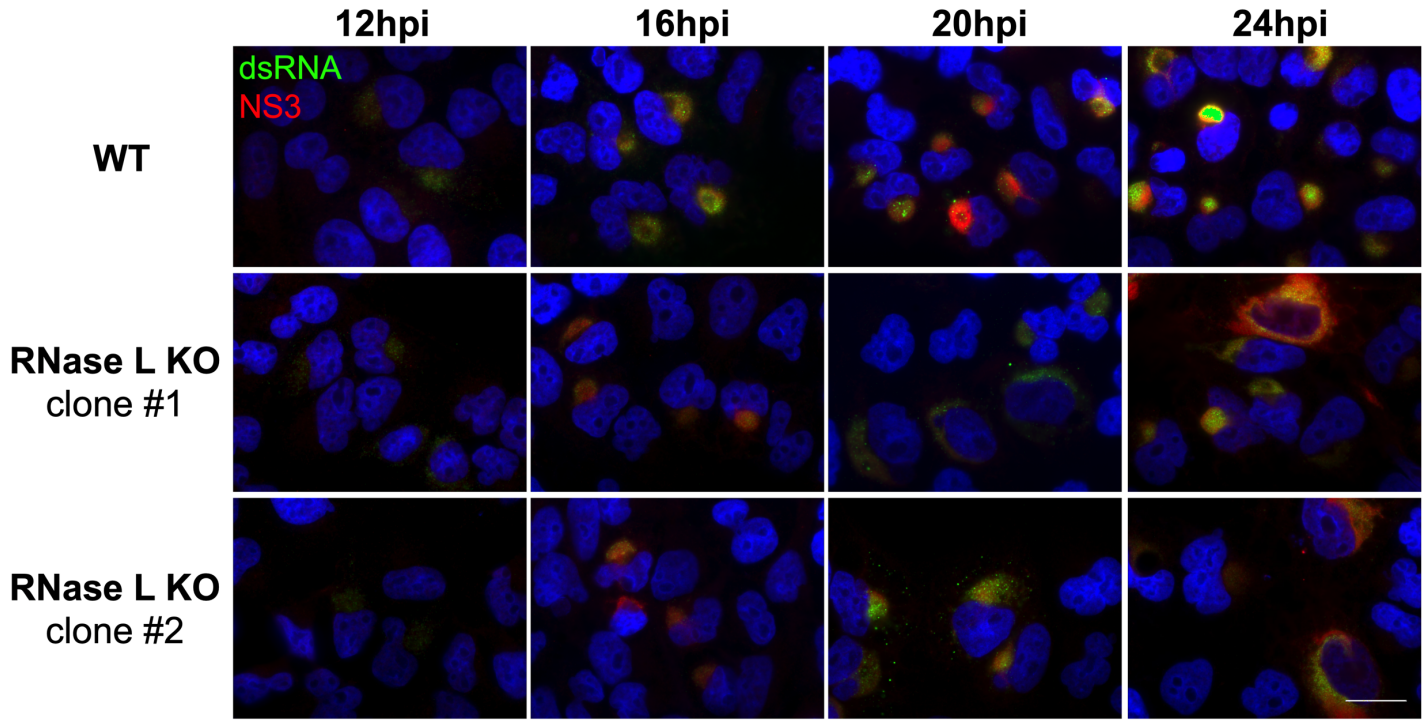

Fig. S1. Loss of RNase L causes ZIKV RNA and protein dissemination. A549 WT cells and two different RNase L clones were infected at an MOI of 1, cells were fixed at 12, 16, 20, or 24hpi for IFA staining for dsRNA (green) and ZIKV NS3 (red), with DAPI (blue) staining of nuclei. Data is representative of at least two independent experiments. Imaged at 100X magnification, scale bar 20μm.

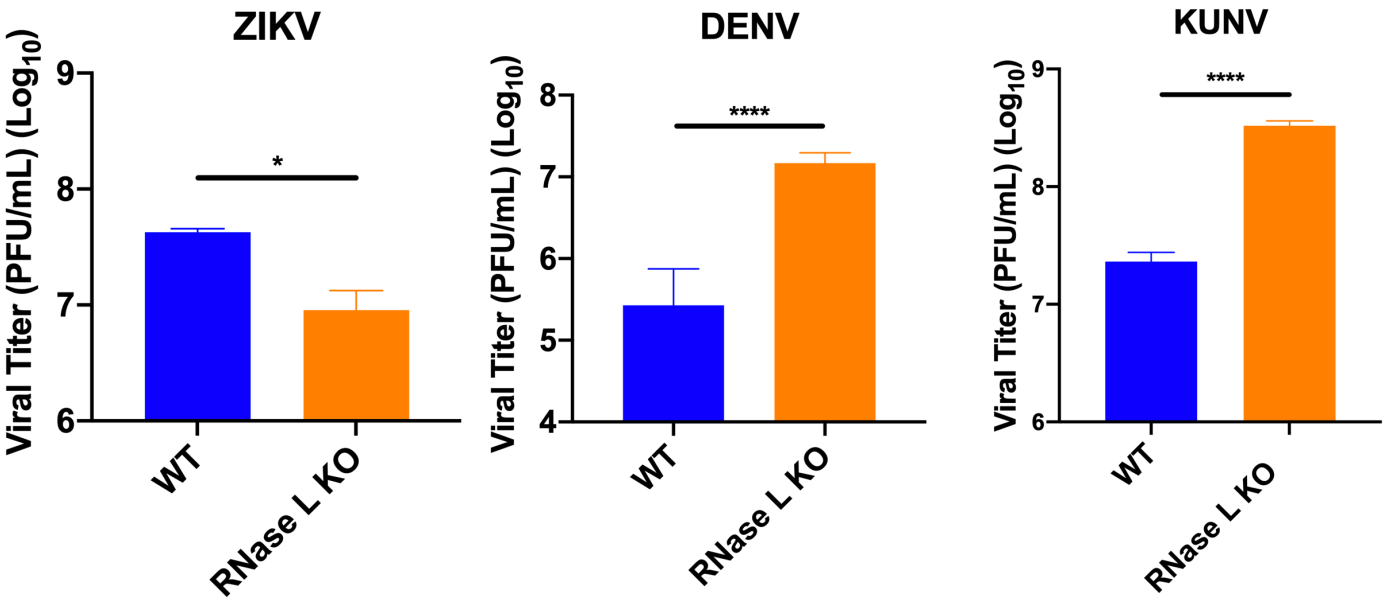

Fig. S2. RNase L antiviral activity inhibits DENV and KUNV production but not ZIKV production. A549 WT or RNase L KO cells were infected with ZIKV, DENV, or KUNV at an MOI of 1, supernatants were harvested at 48hpi for measurement of viral titers by plaque assay, shown as plaque forming units (PFU)/mL virus. Data is representative of at least two independent experiments. Statistical significance was determined by Student's t test, displayed is the mean of three replicates ± SD, *p<0.05, ****p<0.0001.

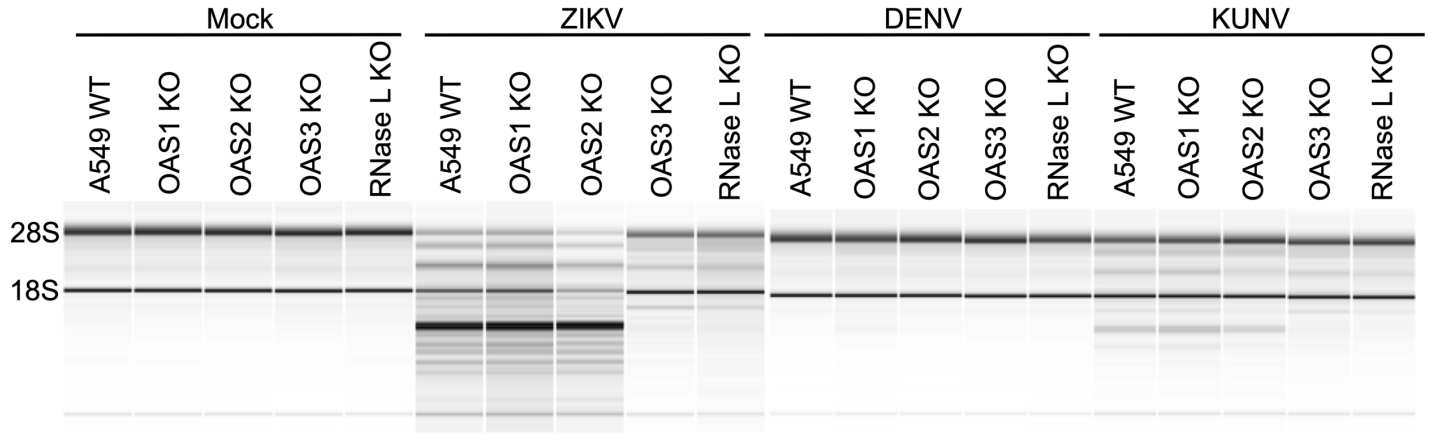

Fig. S3. RNase L activation during ZIKV and KUNV infection is OAS3-dependent. A549 WT, OAS1 KO, OAS2 KO, OAS3 KO, or RNase L KO cells were mock infected or infected with ZIKV, DENV, or KUNV at an MOI of 1 for 48h. 28S and 18S rRNA integrity was analyzed using an Agilent Bioanalyzer. rRNA degradation is displayed as loss of 28S and 18S rRNA integrity, depicted by a lower banding pattern. Data is representative of at least two independent experiments.

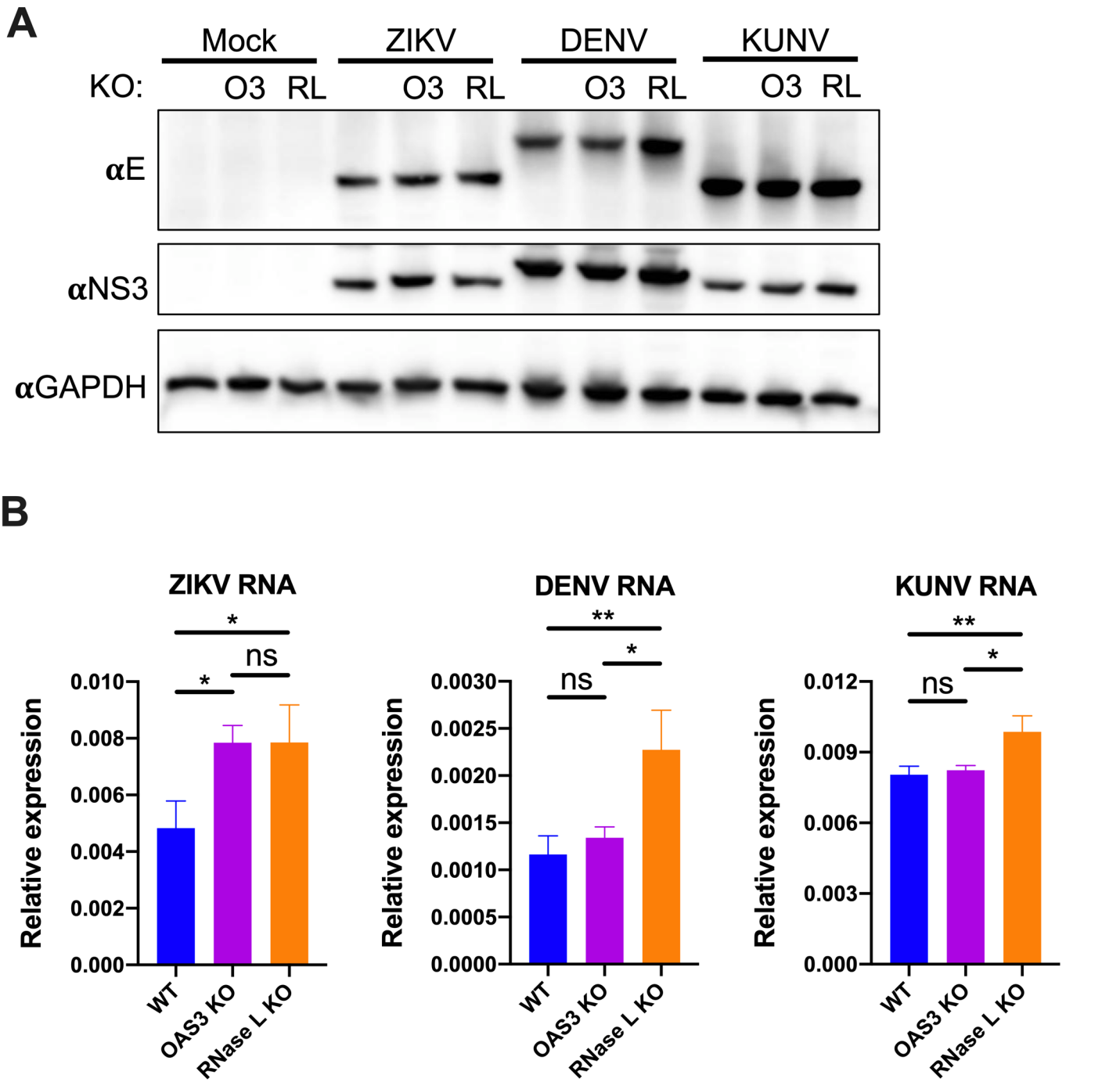

Fig. S4. Total viral RNA and protein in A549 cells. A549 WT, OAS3 KO, and RNase L KO were mock infected or infected with ZIKV, DENV, or KUNV at MOI of 1. (A) Whole cell protein lysates were harvested at 20hpi and total flavivirus E protein, NS3 protein, and GAPDH (loading control) were detected by western blotting. (B) RNA was harvested at 20hpi for RT-qPCR. The cycle threshold values (C_T) were normalized to 18S rRNA to generate ΔC_T values (ΔC_T = C_T gene of interest - C_T 18S rRNA). Three technical replicates were averaged and displayed using the equation $2^{-\Delta CT}$. Data is representative of at least two independent experiments. Statistical significance was determined by one-way ANOVA, displayed is the mean of three replicates ± SD, ns = not significant, *p<0.05, **p<0.01.

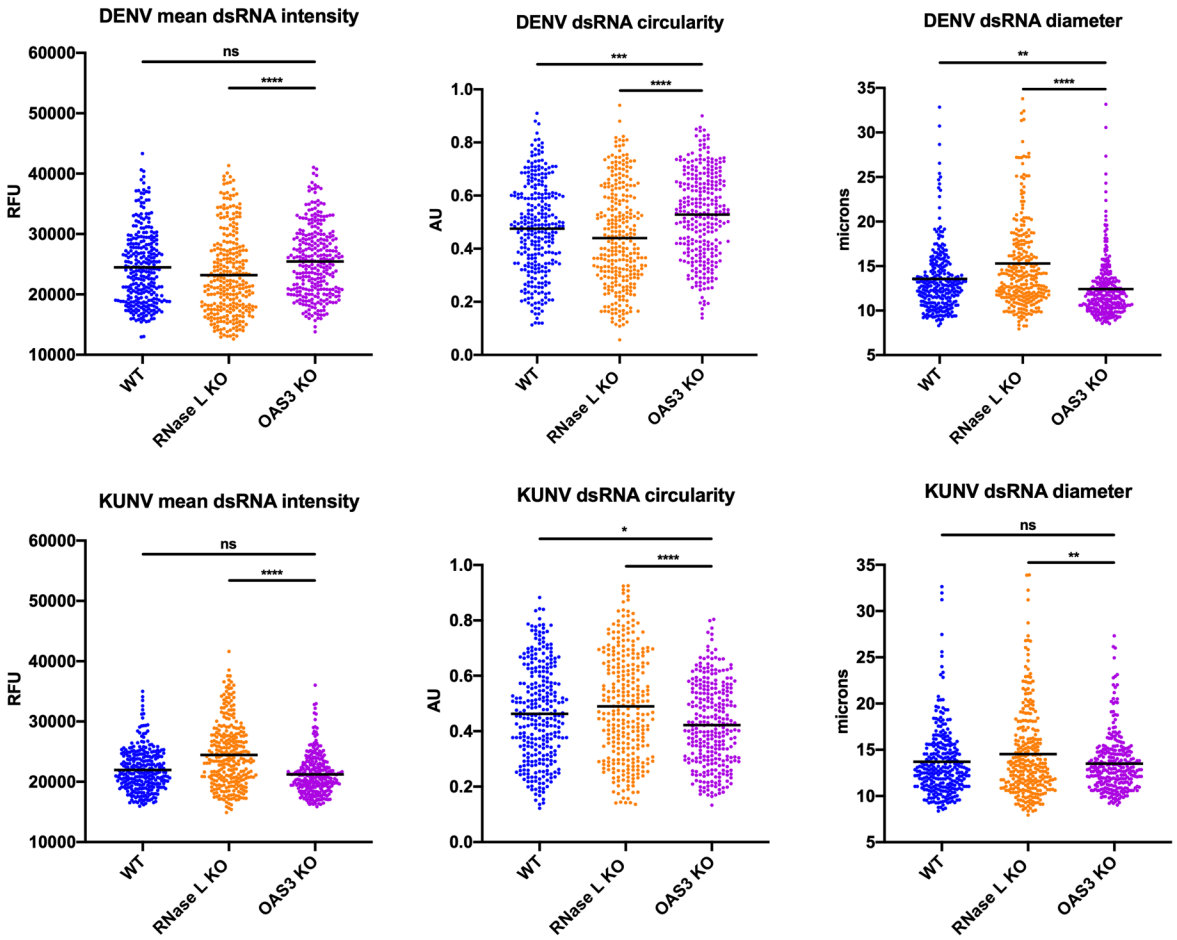

Fig. S5. RNase L has minimal effects on DENV and KUNV dsRNA expression in the absence of OAS3. A549 WT, RNase L KO, or OAS3 KO cells were infected with DENV or KUNV at an MOI of 1, fixed at 20hpi, and stained by IFA for dsRNA for quantification of dsRNA mean intensity, circularity, and diameter. Data is representative of at least two independent experiments. Imaged at 20X magnification. Statistical significance was determined by one-way ANOVA, ns = not significant, *p<0.05, **p<0.01, ***p<0.001, ****p<0.0001.

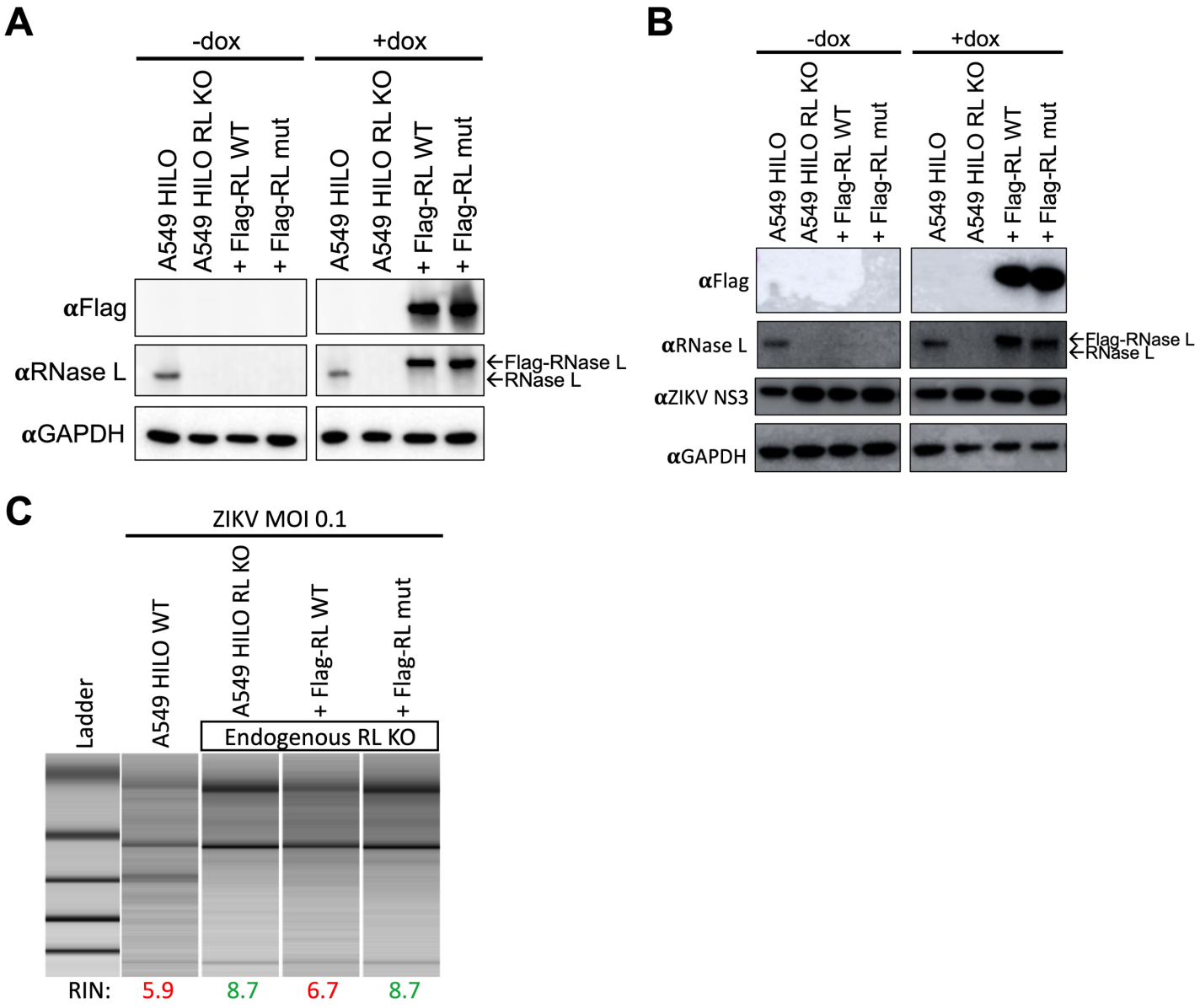

Fig. S6. Generation of A549 HILO RNase L KO cells expressing doxycycline-inducible flag-tagged RNase L WT or RNase L R667A catalytic mutant. A549 HILO cells, A549 HILO RNase L KO cells (RL KO), or A549 HILO RNase L KO cells expressing a doxycycline-inducible flag-tagged RNase L WT (+Flag-RL WT) or R667A catalytic mutant (+Flag-RL mut) were treated with 2μg/mL doxycycline or left untreated. After 24h doxycycline treatment, cells were (A) mock infected or (B) infected with ZIKV at MOI of 2. Protein lysates were harvested at 24hpi and RNase L (endogenous and flag-tagged), ZIKV NS3, and GAPDH (loading control) were detected by western blotting. (C) Doxycycline-treated cells were infected with ZIKV at an MOI of 0.1 for 72h before RNA was harvested and 28S and 18S rRNA integrity was analyzed using an Agilent Bioanalyzer. rRNA degradation is displayed as loss of 28S and 18S rRNA integrity, denoted by RNA integrity number (RIN) quantifying RNA degradation, with 1 being the most degraded and 10 being the most intact.

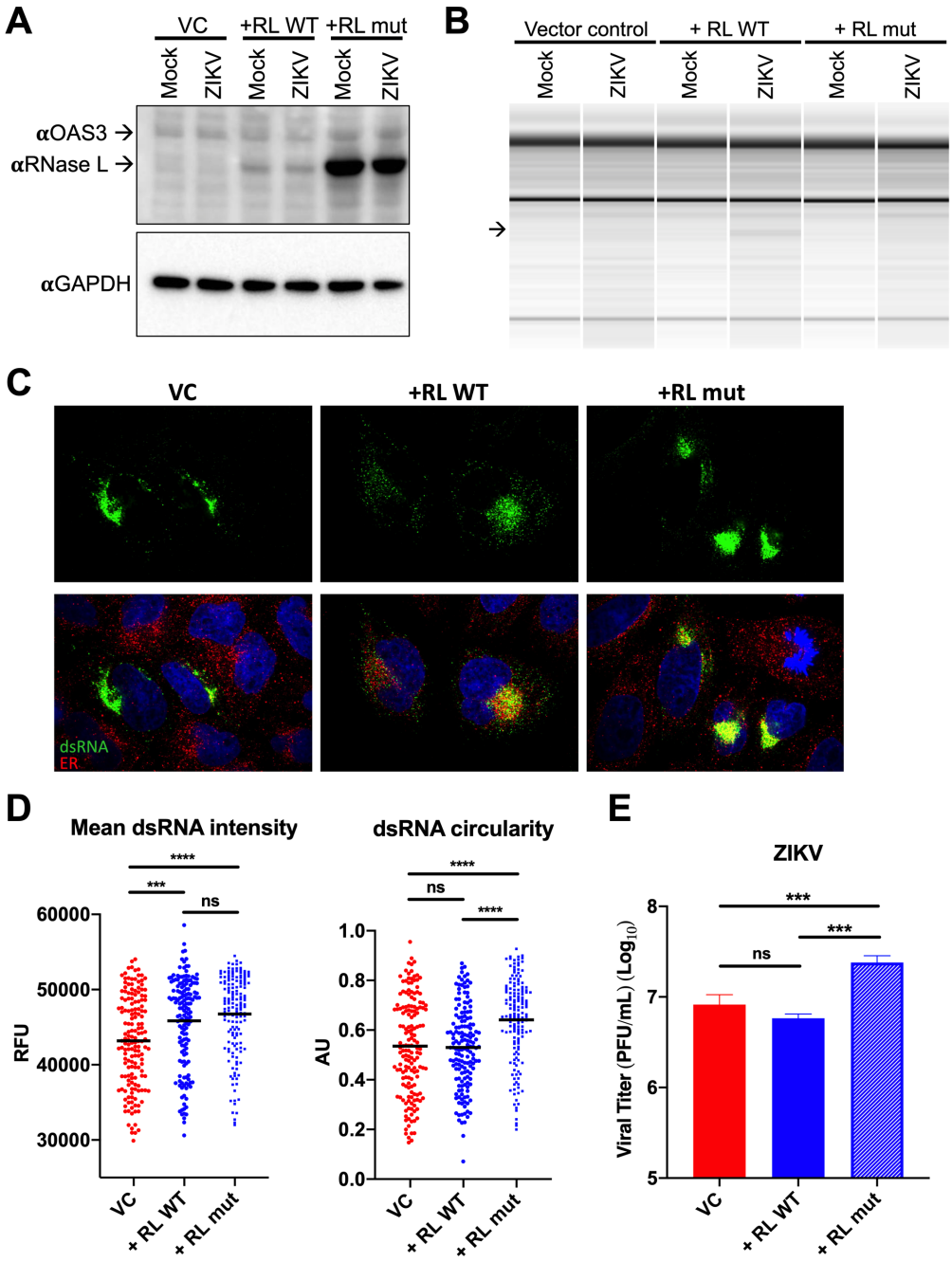

Fig. S7. Expression of RNase L R667A catalytic mutant in HeLa M cells enhances ZIKV RF function and virus production. (A) HeLa M cells expressing empty vector (vector control, VC), RNase L WT (+RL WT), or RNase L R667A nuclease dead mutant (+RL mut) were mock infected or infected with ZIKV at an MOI of 10. Protein lysates were harvested at 24hpi and OAS3, RNase L, and GAPDH (loading control) were detected by western blotting. (B) HeLa M cells were mock infected or infected with ZIKV at an MOI of 5. RNA was harvested 48hpi, and 28S and 18S rRNA integrity was analyzed using an Agilent Bioanalyzer. rRNA degradation is displayed as loss of 28S and 18S rRNA integrity, depicted by a lower banding pattern (black arrow). (C) HeLa M cells were infected with ZIKV at an MOI of 1. At 20hpi, cells were fixed and stained for dsRNA (green) and ER (PDI, red), with DAPI (blue) staining of nuclei. (D) Quantification of ZIKV dsRNA mean intensity and circularity shown in (C). (E) HeLa M cells were infected with ZIKV at an MOI of 0.1, supernatants were harvested at 48hpi for measurement of viral titers by plaque assay, shown as plaque forming units (PFU)/mL virus. Data is representative of at least two independent experiments. Statistical significance was determined by one-way ANOVA, displayed is the mean of three replicates ± SD for replication assays, ns = not significant, ***p<0.001, ****p<0.0001. Imaged at 100X magnification. RFU = relative fluorescence units, AU = arbitrary units.

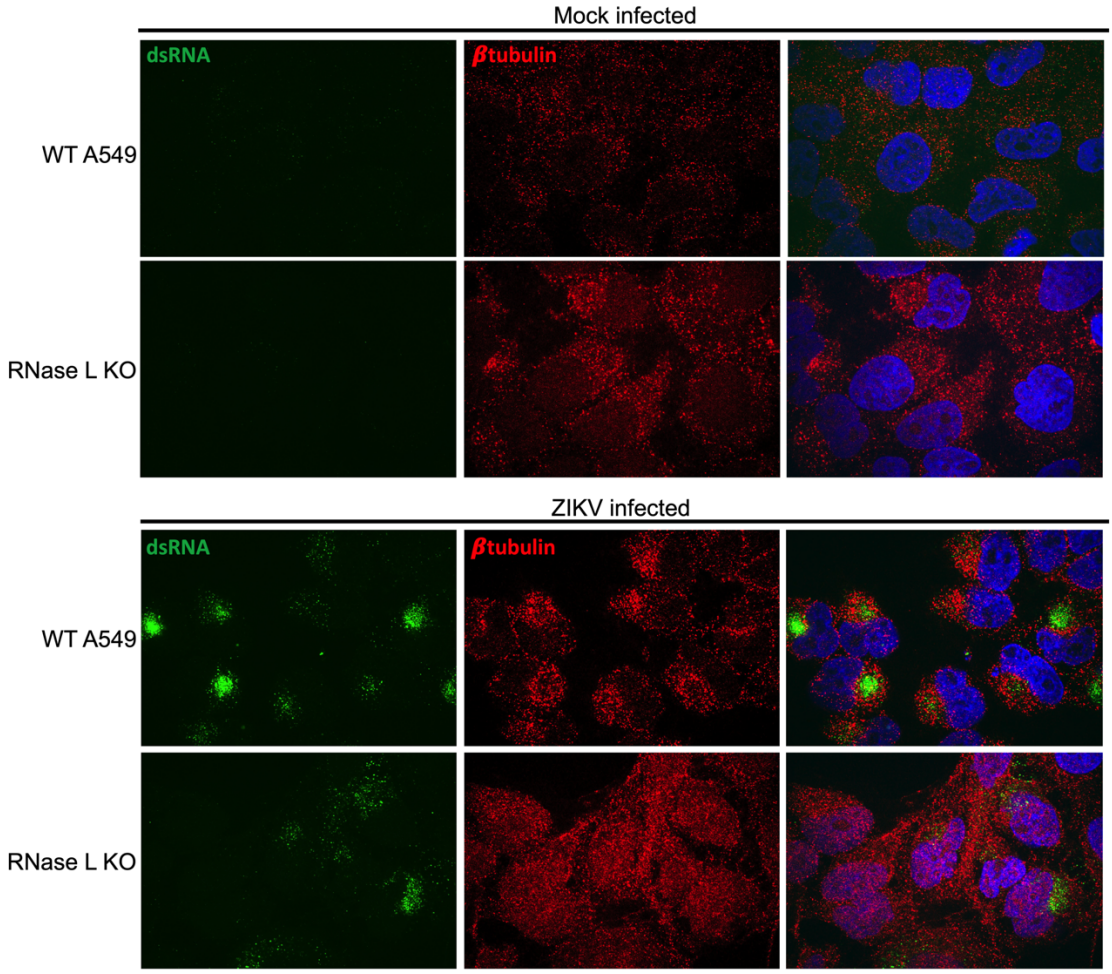

Fig. S8. ZIKV-mediated microtubule rearrangement requires RNase L. A549 WT or RNase L KO cells were infected with ZIKV at an MOI of 1, and fixed for IFA staining cells at 20hpi. Cells were treated with DMSO at 3hpi as part of analysis described in Figure 7. Cells were stained for dsRNA (green) and βtubulin (red), with DAPI (blue) nuclei staining. Data is representative of at least two independent experiments. Imaged at 100X magnification. See also Figure 7.

SI References

1. Y. Li *et al.*, Activation of RNase L is dependent on OAS3 expression during infection with diverse human viruses. *Proc Natl Acad Sci U S A* **113**, 2241-2246 (2016).
2. Y. Li *et al.*, Ribonuclease L mediates the cell-lethal phenotype of double-stranded RNA editing enzyme ADAR1 deficiency in a human cell line. *Elife* **6** (2017).
3. B. Dong, M. Niwa, P. Walter, R. H. Silverman, Basis for regulated RNA cleavage by functional analysis of RNase L and Ire1p. *RNA* **7**, 361-373 (2001).
4. A. A. Khromykh, E. G. Westaway, Completion of Kunjin virus RNA sequence and recovery of an infectious RNA transcribed from stably cloned full-length cDNA. *J Virol* **68**, 4580-4588 (1994).
5. P. Khandelia, K. Yap, E. V. Makeyev, Streamlined platform for short hairpin RNA interference and transgenesis in cultured mammalian cells. *Proc Natl Acad Sci U S A* **108**, 12799-12804 (2011).
6. J. N. Whelan, Y. Li, R. H. Silverman, S. R. Weiss, Zika Virus Production Is Resistant to RNase L Antiviral Activity. *J Virol* **93** (2019).
7. A. Zhang *et al.*, RNase L restricts the mobility of engineered retrotransposons in cultured human cells. *Nucleic Acids Res* **42**, 3803-3820 (2014).
8. Y. Xiang *et al.*, Effects of RNase L mutations associated with prostate cancer on apoptosis induced by 2',5'-oligoadenylates. *Cancer Res* **63**, 6795-6801 (2003).
9. L. Zhao *et al.*, Antagonism of the interferon-induced OAS-RNase L pathway by murine coronavirus ns2 protein is required for virus replication and liver pathology. *Cell Host Microbe* **11**, 607-616 (2012).
10. E. Gusho *et al.*, Murine AKAP7 has a 2',5'-phosphodiesterase domain that can complement an inactive murine coronavirus ns2 gene. *MBio* **5**, e01312-01314 (2014).
11. C. S. Thakur, Z. Xu, Z. Wang, Z. Novince, R. H. Silverman, A convenient and sensitive fluorescence resonance energy transfer assay for RNase L and 2',5' oligoadenylates. *Methods Mol Med* **116**, 103-113 (2005).
12. M. Cortese *et al.*, Ultrastructural Characterization of Zika Virus Replication Factories. *Cell Rep* **18**, 2113-2123 (2017).
13. B. Dong, R. H. Silverman, 2-5A-dependent RNase molecules dimerize during activation by 2-5A. *J Biol Chem* **270**, 4133-4137 (1995).
14. H. J. Stahla-Beek *et al.*, Identification of a novel antiviral inhibitor of the flavivirus guanylyltransferase enzyme. *J Virol* **86**, 8730-8739 (2012).